A Control Strategy for Integration of a PEMFCS to a Distribution Grid

Christina N. Papadimitriou and Nicholas A. Vovos, *Senior Member, IEEE*

***Abstract*-- In order to integrate a proton exchange membrane type (PEM) fuel cell system (FCS) to a distribution system, this paper proposes a local controller for providing primary frequency control and local bus voltage support. The FCS has been designed to operate in the distribution system either this is connected to the mean voltage side or it is disconnected and operated in stand-alone mode. The FCS is connected to a weak distribution grid to study the system performance under local disturbances. The response of the system is recorded under a severe step load change using MATLAB software and proves a good performance of the system.**

***Index Terms*—Distributed Generation, frequency control, Fuel cells, fuzzy logic, voltage control**

I. Introduction

The growth of Distributed Generation (DG) in the distribution grid is expected to play an important role in the power generation in the near future. Until now, penetration of DG in conventional systems is limited in order that the systems overcome emergency situations with the usual procedure. Also, in weak distribution grids high DG penetration results in voltage rise problems, as thoroughly explained in [1], due to the Distribution System Operator (DSO) policy for DG to "fit and forget" requiring only operation at a fixed power factor. This policy fails to integrate the DG to the system and exploiting its capability to mitigate such effects. It's a strong belief, though, that DG can provide ancillary services such as reserves and voltage support under local disturbances providing the demanded active and reactive power by the critical loads.

In [2] and [3] hybrid systems of fuel cell-battery has been presented and efforts have been made in order to regulate the fuel cell and the battery bank power to the dc side demand. In these cases, the hybrid systems operate in stand-alone mode without interfacing with an ac system.

In order to integrate DG to the grid, this paper proposes a fuzzy based local controller for a proton exchange membrane type (PEM) fuel cell system (FCS) combined with a battery bank providing primary frequency control and local bus voltage support. Under this operation philosophy DG must support grid for local disturbances, as central generation station support high voltage systems in the transient period. In the control scheme presented here the hybrid system power covers both the ac and dc side power demand. This is because the FCS has been designed to operate either the distribution system is connected to the mean voltage side or it is disconnected and operates in stand-alone mode. The battery bank delivers power only in the transient period and in steady state the FCS provides the overall power needed. The hybrid system is connected to a weak distribution grid to study the system performance under the worst conditions. The response of the system is recorded under a severe step load change, using MATLAB software. It is expected that when a steady state will be reached, the DSO with a secondary control effort should coordinate DG to optimize operation minimizing active power losses and maintaining flat voltage profile.

In the following section II, the simulation system is described and analyzed. In section III the local controller and its components are analyzed thoroughly. The simulation results are recorded and analyzed in the section IV. The section V concludes the paper.

II. Simulation System Analysis

The overall system configuration is shown in Fig.1. The FCS basically comprises of the stack of the cells, a dc-motor, a compressor and a tank of pure hydrogen. The FCS's electrical output is connected to the chopper 1 so that the output dc voltage is boosted. At the output of the chopper 1 is a battery connected in order to support dc voltage and FCS's performance under fast load changes. The chopper 2 determines through its duty ratio the power that the dc-motor of the FCS absorbs and therefore the air flow supplied by the compressor to the FCS. According to the pressure variation of the supplied air, the supplied hydrogen is regulated and this regulates the output power of the FCS. The dc-side interfaces with the ac-side through a voltage source inverter (VSI). An L-C filter is located at VSI's output followed by a step-up transformer. At the point of common coupling (PCC) a passive load and a weak distribution grid are connected. More details for individual devices are given in the following.

A. PEMFCS

The adopted mathematical model of the FCS is fitted to this paper requirements. Since the FCS is designed

C. N. Papadimitriou is post-graduate student at the Electrical and Computer Engineering Department, University of Patras, 26500 Rion, Patras, GREECE (corresponding author to provide phone: 00302610454134; fax: 00302610996803; e-mail: chpapanetwork@ gmail.com).

N. A. Vovos is professor at the Electrical and Computer Engineering Department, University of Patras, 26500 Rion, Patras, GREECE. (e-mail: N.A.Vovos@ece.upatras.gr).

978-1-4244-2235-7/09/$25.00 ©2009 IEEE

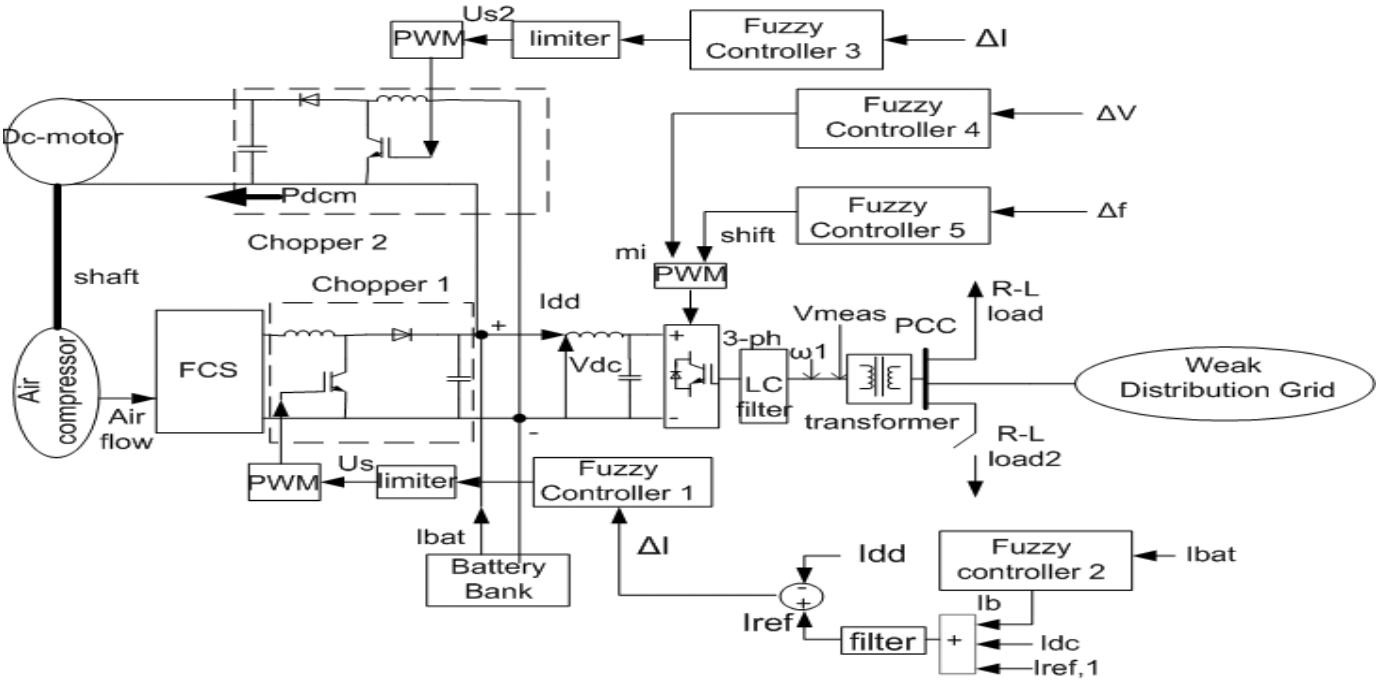

Fig. 1 Configuration of the simulation system.

to operate either the distribution system is connected or disconnected from the mean voltage system, it has to be self-powered meaning that every auxiliary components of the FCS must be supplied by the FCS power and this is especially applied for the air flow compressor. The dc motor drives the compressor through a solid shaft. Controlling the electric power that is supplied by the FCS to the dc-motor, the compressor speed changes regulating the air flow feeding the FCS and therefore the oxygen flow in the cathode manifold. For the anode supply system it is assumed that a tank with compressed hydrogen is available and the hydrogen flow in the anode is adjusted to the air pressure in the cathode using a valve. About other transient phenomena that take place in the FCS such as thermal dynamics, membrane hydration and "double-layer charging effect", the following are assumed. As the study period of the system lasts a few seconds the thermal dynamics are neglected because of their large time constant of 10^2 sec and therefore the stack temperature is assumed to be constant (80^o C) throughout the simulation [4]. The membrane hydration has a transient phase of about 10 sec and therefore the membrane of the PEMFCS is assumed to be fully humidified. Also, the "double-layer charging effect" has been neglected taking into account that the time constant is only 10^{-19} seconds for a single fuel cell [5].

B. Chopper 1

The role of this chopper is not only to boost the FCS output voltage to a certain exploitable level ([6], [7]) but also to regulate the FCS's output power to the ac and dc system required power, without exceeding the FCS capabilities.

C. Battery

Since the FCS has low dynamic response, the battery is covering the fast load changes and the FCS oxygen starvation is avoided. In addition, when our system reaches steady-state, the battery current is forced to zero in order that the FCS supplies the whole demanded power. Battery also supports dc voltage as it keeps the dc voltage deviations into certain limits.

The model of the battery used in the study is adopted by the MATLAB software library (Fig.2) and is parameterized according to the system requirements. The battery type and its parameters are given in the appendix.

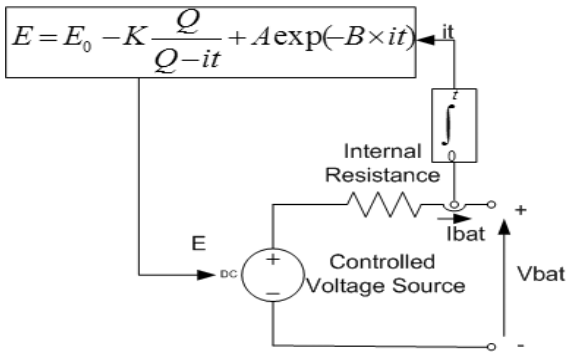

Where: E=No load voltage(V)
Eo=Constant voltage(V)
K=polarization voltage(V)
Q=Battery capacity(Ah)
A=exponential voltage(V)
B=exponential capacity(1/Ah)

Fig. 2 Equivalent circuit of the modeled battery.

D. Chopper 2

The chopper 2 (Fig. 1) controls the supplied dc power to a dc motor that drives a compressor which controls the air flow in the cathode. Therefore the rate of change of the power at the output of the FCS is limited by the overall inertia of the compressor and the motor. In our study, the hydrogen flow is regulated to the oxygen flow through a simple PI controller. The indication of an oxygen starvation is the excess oxygen ratio λ_{O2} which is the ratio of oxygen supplied to oxygen used in the cathode. The optimum value of λ_{O2} is taken equal to 2 where for our chosen FCS the net deliverable power is about maximum. [5]

E. AC side

Through the VSI the active and reactive power supplied to the ac-side are controlled independently. An L-C filter was designed in order to chop the higher harmonics. At the PCC the distribution system has a short circuit capacity equal to 0.2 and an X/R ratio equal to 0.5.

III. LOCAL CONTROLLER ANALYSIS

Because of the non linearity of the system the fuzzy logic was applied in order to control the requisite quantities. The local controller consists of 5 different fuzzy controllers (Fig. 1) that force the hybrid system to provide primary frequency control and local bus voltage support under local disturbances. In the following subsections the input and output signals and the logic of each controller are explained.

A. Chopper 1 Control

The proposed controller integrates the FCS to the distribution grid operation. The chopper 1 control includes the fuzzy controller 1 and the fuzzy controller 2.Through the fuzzy controller 1 that regulates the duty cycle of chopper 1, the system contributes to primary frequency control, supplies the demanded power by the dc-motor and forces the battery supplying current to zero in steady-state. The reference current I_{ref} (Fig.1) for this controller is the sum of three currents. The one $I_{ref,1}$ is created from the sum of a steady state power value Po and the sum of the power variations $\Sigma\Delta P$ according to a power droop, given by $\Delta P=-k*(\omega_1-\omega_{ref})$. The value of the coefficient k is set equal to 2 after tests in our study system. So the Iref, 1 is created according to the following equation $I_{ref,\ 1}= (Po+\Sigma\Delta P)/Vdc$. This current ensures that the active output power of the FCS fits the new demand of the distribution grid. The second reference current I_{dc} is created according to the measured absorbed power of the dc motor, $I_{dc}=P_{dcm}/V_{dc}$ and ensures that the FCS covers the dc motor power. The third I_b is the output of the fuzzy controller 2 whose input is the measured battery bank current and ensures that the battery bank supplying current is forced to zero in steady state. The input of the fuzzy controller 2 is the measured current of the battery I_{bat}. In steady state and when a charging of the battery is asked from the monitoring system, the reference I_b takes a constant value equal to the charging current of the battery. The described creation of the reference current I_{ref} ensures that in transient period the load changes are covered by the FCS (inside its capability) and the rest required load power is covered automatically by the battery. The error between the I_{ref} and the dc current measured at the output of chopper 1, I_{dd}, drives the fuzzy controller 1. The output of the fuzzy controller 1 is the deviations of a signal U_s whose sum create the Us signal which is used in the PWM method [8] applied on the switch of the chopper 1 and determines its duty cycle. This signal must not exceed the FCS capabilities and this is ensured by the limiter at the output of the fuzzy controller 1.After the input and output signals were mentioned, the logic of each controller is explained in the following. When I_{bat} is positive the output of the fuzzy controller 2 is positive and is added in order to build the I_b signal. When I_{bat} is negative, a negative output of fuzzy controller 2 is added to the I_b value. When the measured current of the battery bank is zero the I_b has reached its steady state value. When the I_{dd} value is lower than the reference signal value, the duty cycle of the chopper 1 augments. The opposite happens when the I_{dd} is greater than the reference value.

B. Chopper 2 Control

The fuzzy controller 3 of the chopper 2 regulates the supplied air flow by controlling the dc voltage of the dc motor and ensures that the FCS provides the power demanded by the system without oxygen starvation. The input signal of this controller is the same as in fuzzy controller 1. The output of the fuzzy controller 3 is the deviations of a signal U_{s2} whose sum builds the signal U_{s2} used in the PWM method applied on the switch of the chopper 2 and determines its duty cycle. When the I_{dd} value is lower than the reference signal value, the duty cycle of the chopper 2 augments and the air flow to the cathode augments too. The opposite happens when the I_{dd} is greater than the reference value.

C. VSI Control

The VSI control includes the fuzzy controller 4 and the fuzzy controller 5.

The control of the reactive power is achieved through the modulation index of the PWM method whose value is determined by the fuzzy controller 4. The input of this controller is the error between the reference voltage and the measured voltage at the VSI output. The output of the fuzzy controller 4 is the deviations of the modulation index signal whose values are added together in every simulation step in order to comprise the m_i value at steady state. When the measured voltage is lower than the reference value the m_i increases and the opposite happens when the measured voltage is greater than the reference value. The m_i value is constant when the error between the measured and the reference value of the voltage becomes equal to zero.

The control of the active power is achieved through the shift of the phase angle of the sinusoidal reference signal of the PWM method. The fuzzy controller 5 determines the shift value. The error between the measured frequency at the VSI output and the reference frequency value is used in a droop equation written in the previous section forming the input of this controller. The output of the fuzzy controller 5 is the deviations of the shift signal whose values are added together

in every simulation step in order to comprise the shift value at steady state. When the measured frequency is lower than the reference value the shift value increases in order that the dc side supplies more active power. The opposite happens when the measured frequency is greater than the reference value. When the measured frequency equals to the reference value, the input and the output of the fuzzy controller 5 becomes zero and the shift signal has a constant value.

IV. CONTROL PERFORMANCE AND RESULTS

The data for the system of Fig.1 are given in the appendix. In steady state, the R-L load absorbs its nominal active and reactive power. The grid feeds almost the 2% of the active power and the 0% of the reactive power of the load. The rest 98% of the demanded active power and the whole reactive power is fed by the hybrid system. A step load change was imposed to the system at 0.9 sec by connecting the R-L load 2 to the system and the hybrid system provides primary frequency control and local bus voltage support. Some representative results are shown in Figs. 3-13.

In Fig. 3 the frequency drops at 0.9 sec due to the unbalance of the active power in the system and returns to its nominal value after some oscillations within almost 0.4 sec. In Fig. 4 the hybrid system, forced by the VSI controller, provides the demanded active power to the system in order to restore the frequency signal to its nominal value. The hybrid system supplies almost the 85% of the demanded power and the system reaches a new steady state within 0.9 sec. In Fig. 5 the supplied active power to the R-L load is presented. In steady state the load consumes its nominal active power. At 0.9 sec, when the local disturbance is applied, the absorbed active power by the R-L load decreases and it is restored within 0.9 sec as well. The small static error from the nominal value that is observed lies within acceptable limits. In Fig. 6 the supplied active power to the R-L load 2 is presented. In Fig. 7 the active power that the weak distribution grid supplies is presented. At the time of the applied disturbance, the grid tries instantly to cover the unbalance of the active power in order to restore the frequency signal. In the new steady state it is shown that it supplies the rest 15% of the whole demanded active power. The oscillations that appear in the measured active power signals come from the fact that the signals of voltage and current that are used to the power calculations aren't free of harmonics.

In Fig. 8 the voltage drops at 0.9 sec due to the unbalance of the reactive power in the system and returns to its nominal value after some oscillations within almost 0.9 sec. After tests made in our system, is established that a shorter settling time of the VSI controller leads the system to instability. A small static error from the nominal voltage that is observed lies within acceptable limits. In Fig. 9 the hybrid system, forced by the VSI controller, provides the demanded reactive power to the system in order to restore the voltage signal to its nominal value. In the new steady state, the hybrid system supplies the whole demanded reactive power by the loads and supplies the weak distribution grid too, as it is shown in Fig. 10. In Fig. 11 the supplied reactive power to the R-L load is presented.
In steady state the load consumes its nominal reactive power.

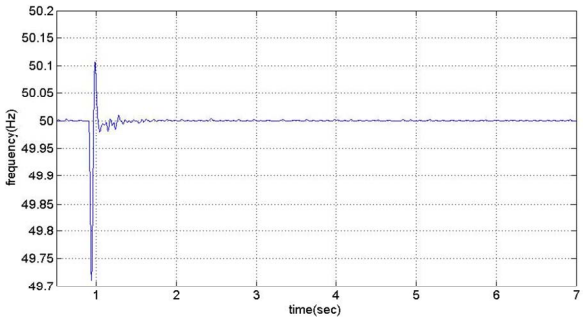

Fig. 3 The measured frequency at the VSI output.

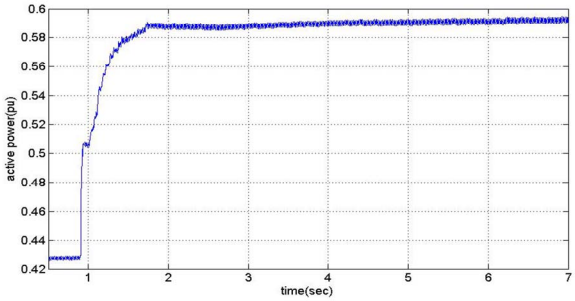

Fig. 4 The measured active power at the VSI output in pu.

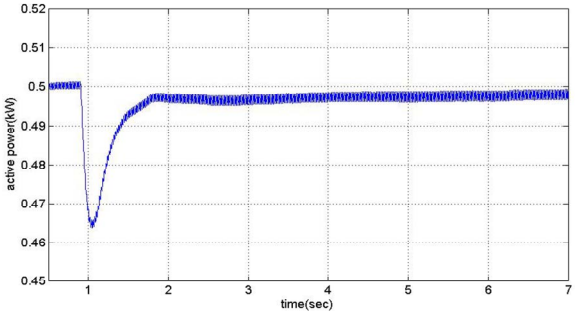

Fig. 5 The supplied active power to the R-L load in pu.

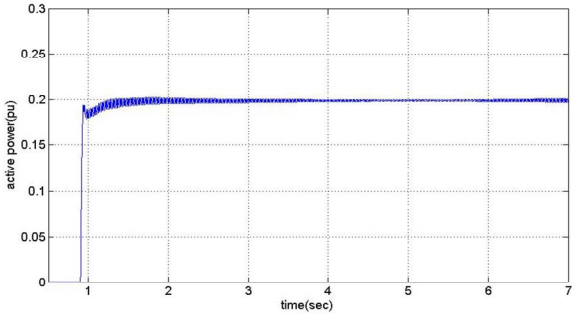

Fig. 6 The supplied active power to the R-L load 2 in pu.

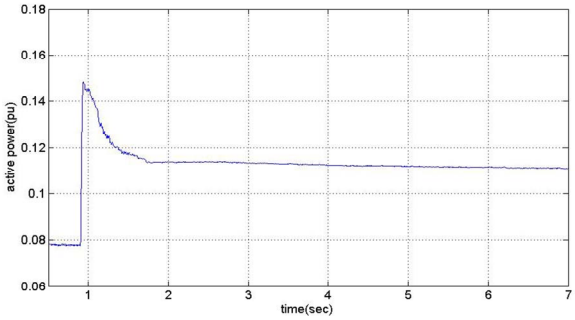

Fig. 7 The supplied active power by the weak distribution grid in pu.

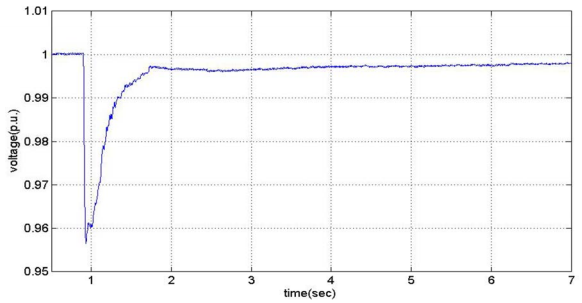

Fig.8 The measured voltage at PCC in pu.

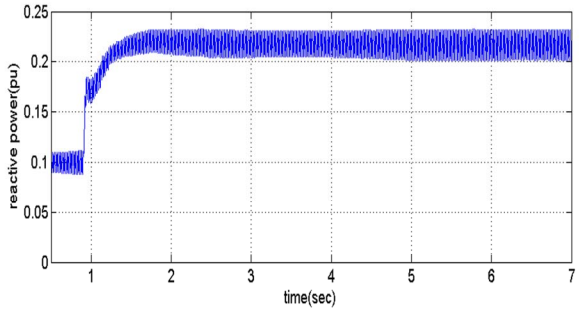

Fig. 9 The measured reactive power at the VSI output in pu.

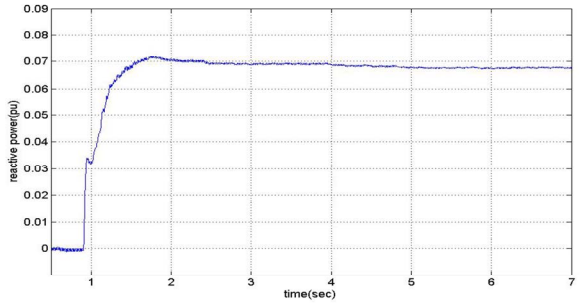

Fig. 10 The absorbed reactive power by the weak distribution grid in pu.

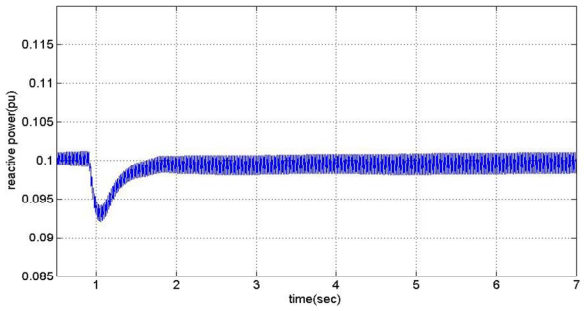

Fig. 11 The supplied reactive power at the R-L load in pu.

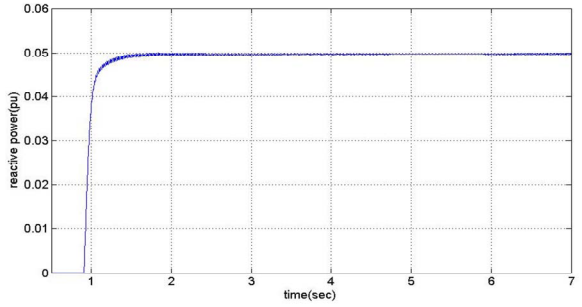

Fig. 12 The supplied reactive power at the R-L load 2 in pu.

At 0.9 sec, when the local disturbance is applied, the absorbed reactive power by the R-L load decreases and it is restored within 0.9 sec as well. In Fig. 12 the supplied reactive power to the R-L load 2 is presented. So, the hybrid system supports the weak distribution grid by providing reactive power. The oscillations that appear in the measured reactive power signals come from the same fact that already mentioned.

The Figs.13-15 refer to the hybrid system and its operation philosophy can be easily excluded. In Fig. 13 the power supplied by the battery bank is presented. In steady state the FCS supplies the 98% of the demanded power as mentioned before and the battery doesn't contribute.

At 0.9 sec, when the local disturbance is imposed the battery bank provides almost instantly the demanded power due to its fast dynamics. So, in the time interval of almost 1 sec, after the local disturbance, the battery bank is the device that mainly tries to restore the unbalance of the active power of the system with the help of the VSI controller. After almost 6 sec the battery current is forced to zero with the help of fuzzy controllers 1 & 2 and thus the power that

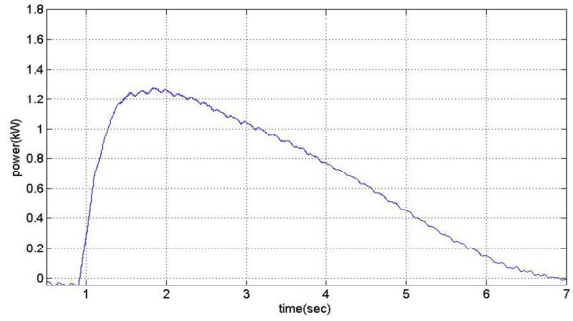

Fig. 13 The delivered power by the battery bank in steady state and in transient period.

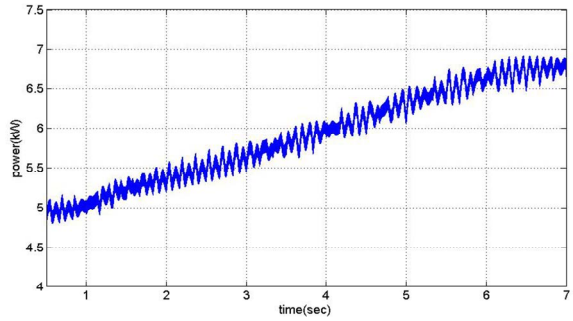

Fig. 14 The FCS delivered power in steady state and in transient period.

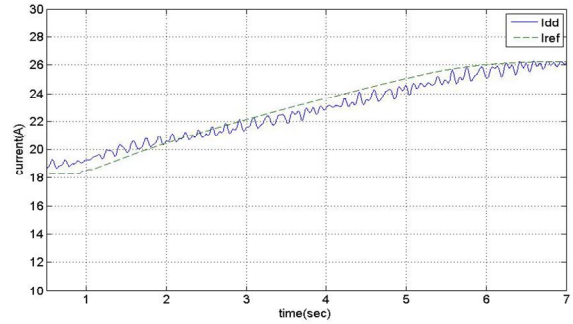

Fig. 15 The signals Idd and the Iref plotted in the same graph.

supplies returns to zero too. In Fig. 14 the delivered power of the FCS is shown. After the local disturbance, the FCS due to its slow dynamics, is slowly forced (due to technical limitations) by the chopper 1 controllers to provide the whole demanded power within 6 sec. It has to be reminded that, in steady state the FCS supplies not only the demanded power by the ac side but also the demanded power by the dc-motor. In Fig. 15 the measured current at Chopper 1 output and the current reference value are plotted in the same graph proving the good performance of Chopper 1 controller.

During the simulation tests, the currents through the IGBTs of the bridge and the voltage across them were measured in order to define their ratings. The peak current that a device has to hold is 30 A and the voltage is 255 V. So, the IGBTs have to be chosen according to the mentioned values.

V. CONCLUSION

This paper proposes a control system to integrate a PEMFCS to the distribution system. The simulation results prove that the PEMFCS can provide auxiliary services to the distribution grid including primary frequency control and local bus voltage support. After a severe step load change, the system behavior was analyzed and revealed good performance. It has to be emphasized that the decentralized control proposed here for DG complements a centralized control that in steady state using a load flow for the distribution system decides for the steady state operation point of each DG in order to optimize grid's performance. The coordination of the DG to move to the demanded operation point by the centralized controller is a similar task with the high voltage system when they forced to operate in optimum dispatch strategy.

APPENDIX

FCS PEM: 10 kW, 150 cells, 100A, 100V, cell active area: 280cm^2.
AC system: 380 V, 50 Hz, base p.u.:10 kW, 380 V.
R-L load : 5kW, 1kVar, 380 V
R-L load 2: 2kW, 0.5kVar, 380 V
dc-motor: 1 hp, 300 V, 1750 rpm, field: 150 V
battery bank: 210 HV Nickel-Metal Hybride cells of 1.2 V, 2 Ah , 250 V.
transformer: 10kVA, 170:380 V, 50 Hz

VI. REFERENCES

[1] C. L. Masters, "Voltage rise: The big issue when connecting embedded generation to long 11 kV overhead lines", Inst. Elect. Eng. Power Eng. J., vol. 16, no.1, pp. 5-12, Feb 2002.

[2] C. Wang, M. H. Nehrir, "Load Transient Mitigation for Stand-Alone Fuel Cell Power Generation Systems", IEEE Trans on Energy Conversion, vol. 22, no.4, pp.864-872, Dec. 2007.

[3] P. Thounthong, S. Rael, and B. Davat, "Control Algorithm of Fuel Cell and Batteries for Distributed Generation System", IEEE Trans on Energy Conversion, vol. 23, no.1, pp.148-155 March 2008.

[4] K. P. Adzakpa, K. Agbossou, Y. Dube,M.Dostie, M.Fournier, and A. Poulin ,"PEM Fuel cells Modeling and Analysis Through Current and Voltage Transient Behaviors", IEEE Trans on Energy Conversion, vol. 23, no.2, pp.581-591, June 2008.

[5] J. T. Pukrushpan, A. G. Stefanopoulou, H. Peng, "Control of Fuel Cell Power Systems: principles, modeling, analysis and feedback design", Springer, 2004,pp. 15-44.

[6] Kyung-Won Suh and A. G. Stefanopoulou, "Coordination of converter and fuel cell controllers" Proceedings of the 13th Mediterranean Conference on Control and Automation, Limassol, Cyprus, pp. 563-568, June 27-29, 2005.

[7] Song-Yul Choe, Jong-Woo Ahn, Jung-Gi Lee and Soo-Hyun Baek, "Dynamic Simulator for a PEM Fuel Cell System with a PWM DC/DC Converter", IEEE Trans on Energy Conversion, vol. 23, no.2, pp.669-680, June 2008.

[8] Mohan, Undeland, Robbins, " Power Electronics: Converters, Applications and Design", Wiley, 2003, pp. 161-200.

VII. BIOGRAPHIES

Christina N. Papadimitriou was born in Arta, Greece in 1984. She obtained her diploma in Electrical and Computer Engineering from the University of Patras, Greece in 2006, where she is currently working towards her Ph.D. Degree. Her main research interests include renewable energy sources, power quality, computer applications in power system analysis and intelligent control.

Nicholas A. **Vovos** (M76, SM95) was born in Thessaloniki, Greece in1951.He received his diploma and Ph.D. degrees from the University of Patras**,** Greece and the M.Sc. degree from the University of Manchester Institute of Science and Technology (UMIST), England in 1974 1978 and 1975 respectively. He is professor in the Electrical and Computer Engineering Department of the University of Patras and his main fields of interest are the transient stability study of integrated AC/DC systems, FACTS, power quality, and renewable energy sources